

Manipulating Single Neutral Atoms in Optical Lattices

Chuanwei Zhang¹, S. L. Rolston², and S. Das Sarma¹

¹ Condensed Matter Theory Center, Department of Physics,
University of Maryland, College Park, Maryland, 20742 USA

² Department of Physics, University of Maryland, College Park, Maryland, 20742 USA

We analyze a scheme to manipulate quantum states of neutral atoms at individual sites of optical lattices using focused laser beams. Spatial distributions of focused laser intensities induce position-dependent energy shifts of hyperfine states, which, combined with microwave radiation, allow selective manipulation of quantum states of individual target atoms. We show that various errors in the manipulation process are suppressed below 10^{-4} with properly chosen microwave pulse sequences and laser parameters. A similar idea is also applied to measure quantum states of single atoms in optical lattices.

PACS numbers: 03.67.Lx, 03.75.Lm, 03.75.Mn, 39.25.+k

Neutral atoms trapped in optical lattices are excellent candidates for quantum computation because they are well isolated from environment, hereby leading to long coherence times, and easy to use for storing and processing quantum information [1, 2]. In optical lattices, controlled interactions between atoms may be implemented effectively, and highly entangled states of many atoms may be created in a single operational step [3, 4, 5]. More importantly, very efficient schemes for quantum error corrections [6] and fault-tolerant computing [7] can be straightforwardly implemented because of parallel operations in optical lattices [8] and long coherence times.

An outstanding challenge for quantum computation in optical lattices is the selective manipulation and measurement of quantum states of single atoms, because spatial periods of typical optical lattices are shorter than optical resolutions (long wavelength lattices may provide single site addressability [9], but it is difficult to implement Mott insulating states with one atom per site necessarily for quantum computation in such lattices). Single qubit operation is not only a building block of universal quantum computation [10], but is also an essential ingredient for the recently proposed one way quantum computation, where quantum information is processed by performing single qubit rotations and measurements on entangled cluster states [11]. Experimentally, entangled cluster states have been realized for neutral atoms by using controlled cold collisions in spin-dependent optical lattices [4]. Therefore, implementation of single atom manipulation and measurement eventually lead to universal quantum computation in optical lattices.

In this Letter, we show that high fidelity selective manipulation and measurement of single atoms in optical lattices may be achieved with the assistance of focused lasers [12]. Consider a deep two dimensional optical lattice with one atom per lattice site [13]. The logical qubit basis of each atom is formed by two hyperfine states that can be coupled coherently using microwave radiation. The couplings are same for all atoms because of the degeneracy of their hyperfine splittings. In the presence

of spatially varying external fields, the degeneracy may be lifted and single atom manipulation becomes feasible. For instance, individual atoms separated around $2.5\mu\text{m}$ have been selectively addressed in an experiment using magnetic field gradients [14], but such a method is not practical for atoms separated by a half-wavelength of typical optical lattices, where impractically large magnetic field gradients would be required.

The degeneracy of hyperfine splittings may also be lifted in the presence of focused lasers that induce position-dependent energy shifts of hyperfine states (*light shift*) [15] due to the spatial distributions of laser intensities. Through varying intensities and detunings of the focused lasers, we may adjust the difference of hyperfine splittings between neighboring atoms to a regime where microwave radiation affects mainly target atoms, while impact on non-target atoms are strongly suppressed with properly chosen microwave pulse sequences. Various errors in the manipulation process are found to be below 10^{-4} except the spontaneous emission probability of atoms in the focused laser. Finally, we show that the quantum states of individual atoms in optical lattices may also be measured using position-dependent energy shifts of hyperfine states.

We develop the scheme as realistically as possible, and illustrate it using ^{87}Rb atoms, although the technique is applicable to other species as well. Consider ^{87}Rb atoms confined in a two dimensional (xy plane) optical lattice with wavelength $\lambda = 850\text{nm}$. The lattice is ramped up adiabatically to a potential depth $V_L = 50E_r$ such that the Bose-Einstein condensate is converted into a Mott insulating state with one atom per lattice site [13]. Here E_r denotes the recoil energy $E_r = \hbar^2 k^2 / 2m$. Two hyperfine ground states $|F = 1, m_F = -1\rangle \equiv |0\rangle$, and $|F = 2, m_F = -2\rangle \equiv |1\rangle$ are chosen as the logical basis of a single atom qubit at each site.

To manipulate a target atom A , we adiabatically turn on a focused laser that propagates along \hat{z} axis and has the maximal intensity located at A (Fig.1). The focused laser is obtained by passing

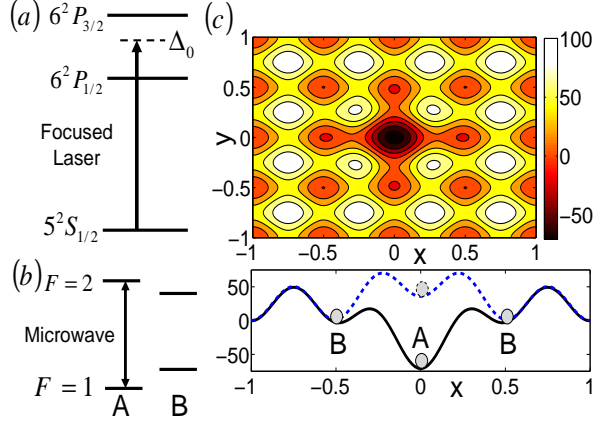


Figure 1: (color online). The scheme for manipulating single atoms in optical lattices using focused lasers and microwave radiation. (a) ^{87}Rb hyperfine structure. Δ_0 is the detuning of the focused laser from the transition $5^2S_{1/2} \rightarrow 6^2P_{3/2}$. (b) Position-dependent hyperfine splittings induced by the spatial distribution of the focused laser intensity. Microwave radiation couple two hyperfine states of atoms. (c) Optical potentials for atoms around the focused laser. The length unit is the wavelength $\lambda = 850\text{nm}$ of the optical lattice. The energy unit is the recoil energy E_r . Top: a 2D plot for atoms at state $|0\rangle$. Bottom: a 1D plot along $y = 0$. Solid and dashed lines for states $|0\rangle$ and $|1\rangle$ respectively.

an initial large Gaussian beam with waist width w through a lens with diameter D and focal length f , and its intensity shows an Airy pattern $I(r) = \frac{I(0)}{G} \int_0^{\frac{D}{2}} r' J_0 \left(k_f r' r / \sqrt{r'^2 + f^2} \right) \exp(-r'^2/w^2) dr'$, where $k_f = 2\pi/\lambda_f$ is the wavevector of the focused laser, $J_0(r)$ is the zero order Bessel function, and $G = \int_0^{D/2} r' J_0(0) \exp(-r'^2/w^2) dr'$. Such an intensity pattern induces position-dependent energy shifts [16]

$$\Delta E_i(r) = \frac{3\pi c^2}{2} I(r) \sum_{j(\neq i)} \frac{\Gamma_j |c_{ij}|^2}{\omega_{ij}^3 \Delta_{ij}} \quad (1)$$

for hyperfine ground states $|0\rangle$ and $|1\rangle$, where c is the speed of light, Γ_j is the decay rate of excited state $|j\rangle$, c_{ij} is the coefficient, ω_{ij} is the frequency, and Δ_{ij} is the detuning of the focused laser for the transition $|i\rangle \rightarrow |j\rangle$. Different polarizations and detunings of the focused laser yield different shifts of hyperfine splittings $|\Delta E(r)| = |\Delta E_1(r) - \Delta E_0(r)|$ between two qubit states. Here we choose a σ^+ -polarized laser that drives the $5S \rightarrow 6P$ transition [17] to obtain a small diffraction limit (Fig.1(a)). The laser induces a red-detuned trap for state $|0\rangle$, but a blue-detuned trap for state $|1\rangle$. The wavelength $\lambda_f \approx 421\text{nm}$ is optimized to obtain maximal ratio between energy splitting of two qubit states and the spontaneous scattering rate [4].

Because of the inhomogeneity of the focused laser intensity, $|\Delta E(r)|$ reaches a maximum at the target atom

A and decreases dramatically at neighboring sites, as shown in Fig. 1. Therefore the degeneracy of hyperfine splittings between different atoms is lifted (Fig.1(b)). In Fig.1(c), the optical potentials V for atoms around the focused laser is plotted. We see that the minimal potential barrier, $\Delta V \approx 20E_r$, occurs for atom B at state $|0\rangle$. The tunneling rate of atom B to the neighboring site A is $\varpi \approx 2\pi J^2/\hbar E_g$ using Fermi's Golden rule, where J is the hopping matrix element and E_g is the energy gap between the initial and final states. In a symmetric optical lattice, E_g is just the on-site interaction between two atoms. The asymmetry of sites A and B yields an energy gap E_g on the order of the trapping frequency of site A, which strongly suppresses the tunneling rate. A rough estimation shows that the tunneling time $1/\varpi$ is about 13s for the parameters in Tab. I.

To avoid excitations of atoms to higher bands of optical lattices, the rising speed of the focused laser intensity should satisfy the adiabatic condition $\hbar |d\Delta E_i(0)/dt| = \xi |\omega_{eg}|^2 / |\langle \Phi_e | \partial V / \partial \Delta E_i(0) | \Phi_g \rangle|$, where ω_{eg} is the energy gap, $|\Phi_g\rangle$ and $|\Phi_e\rangle$ are the wavefunctions of the ground and excited states, and $\xi \ll 1$ is a parameter that determines the degree of the adiabaticity. Because of the high potential barrier for each atom, the wavefunctions and energy gap may be obtained using the harmonic oscillator approximation, and we find $\left| \frac{d\Delta E_i(0)/E_r}{dt} \right| = \xi \frac{8\bar{w}^2 E_r (\Delta V_i(r)/E_r)^{5/4}}{\hbar a_0 r \exp(-2r^2/\bar{w}^2)}$, where $a_0 = \sqrt{\hbar^2/mE_r}$, $\Delta V_i(r)$ is the potential barrier for atom at position r with state $|i\rangle$, and we have approximated the Airy pattern of the focused laser intensity using a Gaussian function with an effective beam waist width \bar{w} . The rising speed is limited by atom B at state $|0\rangle$ that has minimal potential barrier, and is estimated to be $\left| \frac{d\Delta E_0(0)/E_r}{dt} \right| \approx 3.6 \times 10^6 \xi (\Delta V(\lambda/2)/E_r)^{5/4} \text{Hz}$. The total ramping up time is found to be $57\mu\text{s}$ for $\xi = 0.005$, which corresponds to a 10^{-4} probability for excitation to higher bands.

The position-dependent hyperfine splittings induced by the focused laser, combined with microwave radiation, can be used to perform arbitrary single qubit unitary operations on the target atom A. The microwave frequency is chosen to be resonant with the hyperfine splitting of A, and has a $\delta(r) = (|\Delta E(0)| - |\Delta E(r)|)/\hbar$ detuning

Table I: Experimental parameters. $\delta(\lambda/2)$ is the difference of the hyperfine splittings between atoms A and B. For other atoms, δ is slightly larger. τ is the spontaneous emission probability for atoms in the focused laser during the single qubit manipulation process. The units are nm for λ and λ_f , mm for D , f , w , GHz for $\Delta_0/2\pi\hbar$, E_r for V_L , $\Delta E(0)$, $\hbar\delta(\lambda/2)$, $\hbar\omega_0$, and ΔV , 10^{-4} for τ .

λ	V_L	D	f	w	λ_f	$\frac{\Delta_0}{2\pi\hbar}$	$ \Delta E(0) $	$\hbar\delta(\frac{\lambda}{2})$	$\hbar\omega_0$	ΔV	τ
850	50	20	20	20	421	-1209	107	102	12.8	15	6

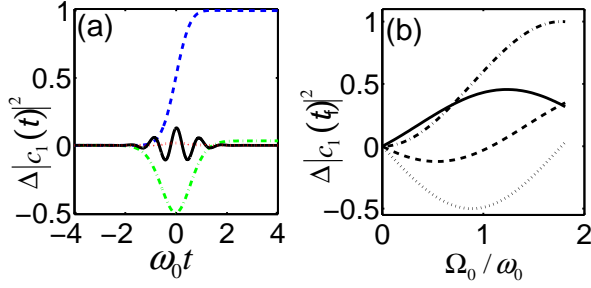


Figure 2: (color online). (a) Time evolution of $\Delta|c_1(t)|^2$ during the microwave pulses. $\Omega_0/\omega_0 = 1.81$. Atoms A (dashed dotted) and B (solid) with initial state $(c_0, c_1) = (\sqrt{\frac{1}{2}}, i\sqrt{\frac{1}{2}})$; atoms A (dashed) and B (dotted) with initial state $(1, 0)$. (b) $\Delta|c_1(t_f)|^2$ is the population variation of atom A after the microwave pulse. Initial states $(1, 0)$ (dashed dotted); $(\sqrt{\frac{1}{2}}, i\sqrt{\frac{1}{2}})$ (dotted), $(\sqrt{\frac{2}{3}}, \sqrt{\frac{1}{4}} + i\sqrt{\frac{1}{12}})$ (dashed), and $(\sqrt{\frac{2}{3}}, \sqrt{\frac{1}{4}} - i\sqrt{\frac{1}{12}})$ (solid).

for non-target atoms (Fig. 1(b)). The coupling between two states $|0\rangle$ and $|1\rangle$ is described by the Rabi equation

$$i \frac{d}{dt} \begin{pmatrix} c_0 \\ c_1 \end{pmatrix} = \begin{pmatrix} 0 & e^{-i\chi}\Omega(t)/2 \\ e^{i\chi}\Omega(t)/2 & -\delta \end{pmatrix} \begin{pmatrix} c_0 \\ c_1 \end{pmatrix}, \quad (2)$$

where Ω is the Rabi frequency and χ is the phase of the microwave. The evolution of the quantum states is equivalent to the rotation of a spin with components $S_z = |c_1|^2 - |c_0|^2$, $S_x = 2\cos\theta|c_1c_0|$, $S_y = 2\sin\theta|c_1c_0|$ on a Bloch sphere [15], where θ is the relative phase between two states. δ is the rotation frequency along \hat{S}_z axis, while $\Omega(t)$ is the frequency along an axis in xy plane whose direction is determined by phase χ . For instance, $\chi = 0$ and $\pi/2$ correspond to rotations along axes \hat{S}_x and \hat{S}_y respectively, and the combination of them may implement arbitrary single qubit unitary operations [1]. In this Letter we focus on $\chi = 0$ although similar results for $\chi = \pi/2$ may be obtained straightforwardly.

To achieve a reliable single qubit rotation with negligible impact on non-target atoms, the microwave Rabi pulse needs to satisfy the following criteria: (i) the variation of the occupation probabilities of state $|1\rangle$ of non-target atoms is extremely small (below 10^{-4}); (ii) the relative phase θ between two qubit states must return to the initial value after the microwave pulse. In the following, we show how a single qubit rotation on the target atom A satisfying these criteria is achieved by using Gaussian shaped rotation pulses together with refocusing pulses.

A Gaussian shaped pulse $\Omega(t) = \Omega_0 \exp(-\omega_0^2 t^2)$ ($-t_f \leq t \leq t_f$) is used to perform single qubit rotation on the target atom A . The effective Rabi frequency in the frequency domain $\Omega(\omega)$ (the Fourier transform of $\Omega(t)$) of this type of pulse shows a Gaussian shaped decay with respect to the detuning δ from the microwave

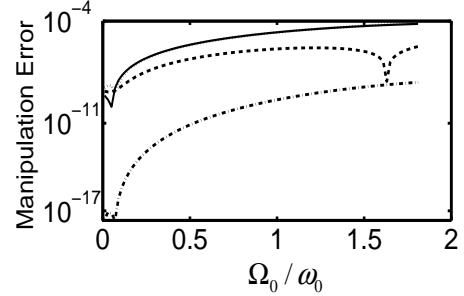


Figure 3: Manipulation error $\epsilon = ||c_1(t_f)|^2 - |c_1(-t_f)|^2|$ for the nearest neighboring atom B . ϵ is smaller for other atoms because they have larger detuning $\delta(r)$. $-7 \leq \omega_0 t_f \leq 7$ in the numerical integration of Eq. (2). Initial states are same as those in Fig. 2(b).

frequency. Because of their large detuning δ , non-target atoms undergo Rabi oscillations with small effective frequencies $\Omega(\delta)$, which strongly suppress the variations of their occupation probabilities.

This scenario is confirmed by numerically integrating Eq. (2) with different initial states and calculating the variation $\Delta|c_1(t)|^2 = |c_1(t)|^2 - |c_1(-t_f)|^2$ of the occupation probabilities at state $|1\rangle$. A small constant $\omega_0 = \frac{1}{8}\delta(\frac{\Delta}{2})$ for the microwave is chosen to avoid large impact on non-target atoms, and different pulse areas are implemented by varying the pulse amplitude Ω_0 , instead of the pulse period $2t_f$. In Fig. 2(a), $\Delta|c_1(t)|^2$ of atoms A and B are plotted with respect to the scaled time $\omega_0 t$. We see large variations of $|c_1|^2$ for atom A after the pulse, which corresponds to a single qubit rotation. In comparison, there are no obvious changes of $|c_1|^2$ for the neighboring atom B . In Fig. 2(b), the total changes of $|c_1|^2$ for the target atom A at time t_f is plotted with respect to Ω_0/ω_0 . We see different pulse areas can be achieved by adjusting Ω_0 .

For the target atom ($\delta = 0$), the time evolution of $|c_1(t)|^2$ can be obtained analytically by solving Eq. (2), which yields

$$|c_1(t)|^2 = (1 - \rho \sin(\eta\Omega_0/\omega_0 + \phi)) / 2. \quad (3)$$

Here $\rho = \sqrt{1 - 4|c_0(-t_f)|^2|c_1(-t_f)|^2 \cos^2\theta(-t_f)}$, $\eta = \omega_0 \int_{-t_f}^t \exp(-\omega_0^2 t'^2) dt'$ and $\phi = \arcsin((1 - 2|c_1(-t_f)|^2)/\rho)$. This expression is in very good agreement with the numerical results presented in Fig. 2.

In Fig. 3, we plot the single qubit manipulation errors for the nearest neighboring atom B with respect to Ω_0/ω_0 . The errors are smaller than 10^{-4} for different Rabi pulse lengths and different initial states. We also perform numerical simulations for many other initial states and find that errors below 10^{-4} are always achieved. The manipulation errors are even smaller for all other atoms because they have larger detuning $\delta(r)$.

The relative phase θ is harder to control than the occupation probability because it can not only vary from 0 to 2π many times with large frequency $\delta(r)$ during the Rabi pulse, but also be easily affected by interaction with the environment that leads to dephasing. To eliminate the variation of θ , we use the following pulse sequence that is similar to the refocusing process in NMR studies [1]. In step (i), we adiabatically ramp up the focused laser, apply a $\alpha/2$ pulse on the target atom A using the Gaussian shaped pulses described above, then adiabatically ramp down the focused laser. In this step, atoms obtain phase variations $\Delta\theta$ determined by their detunings $\delta(r)$ and the dephasing process. In step (ii), we apply a fast resonant π pulse to all atoms that correspond to an angle π rotation along S_x axis. This pulse is called the refocusing pulse. In step (iii) we repeat step (i), and in step (iv) we apply another π refocusing pulse. In step (iii) the effective direction of the rotations along S_z axis for all atoms is reversed from that in step (i) by two refocusing pulses, therefore the phase variation in step (iii) becomes $-\Delta\theta$. These two phase variations cancel each other and the relative phase θ returns to its initial value after the pulse sequence.

In an experiment, a difficult parameter to specify is the spatial distribution of the focused laser intensity that determines the detuning $\delta(r)$, the central parameter of the scheme. However, our scheme requires large $\delta(r)$, not any specific values, therefore not significantly affected by this difficulty. Another important issue in the experiment is the misalignment of the focused laser from the minimum of the optical lattice potential. A small displacement Δx of the focused laser induces a detuning of the microwave scaling as $(\Delta x)^2$ from the hyperfine splitting between two qubit states of the target atoms, and thus reduces the fidelity of the single qubit rotation. For $\Delta x = 1\text{nm}$, we estimate the detuning to be $1.1 \times 10^{-3}\omega_r$. Generally, errors due to small mis-detuning of the microwave may be corrected using composite pulses technology developed in the NMR quantum computation [18].

In the single qubit manipulation, the probability of spontaneous scattering one photon for atoms in the focused laser is estimated to be $\tau = 6 \times 10^{-4}$, which is the worst parameter in the scheme. This parameter is limited by the need for an appropriate vector light shift, which does not allow arbitrarily large detunings.

The energy shift induced by the focused laser is around several hundreds KHz , which is much smaller than the decay rate Γ of excited states and can not be used to selectively measure quantum states of target atoms. To obtain large energy shifts, we transfer the target atom to other magnetic sublevels ($|0\rangle \rightarrow |\bar{1}\rangle \equiv |F=2, m_F=2\rangle$, $|1\rangle \rightarrow |0\rangle$) using several π microwave pulses with the assistance of the focused laser. Then a focused σ^+ -polarized laser resonant with the transition $|\bar{1}\rangle \rightarrow |6^2P_{3/2} : F' = 3, m'_{F'} = 3\rangle$ is applied to detect atoms at state $|\bar{1}\rangle$. In this process, reso-

nant fluorescence is observed if and only if the initial state of the target atom is $|0\rangle$ and the probability to detect an atom yields $|c_0|^2$ of the target atom. In the experiment, a constant $15G$ magnetic field along x -axis may be used to induce about $2\pi \times 42MHz$ Zeeman splitting between states $|1\rangle$ and $|\bar{1}\rangle$, while $2\pi \times 55.8MHz$ between $|6^2P_{3/2} : F' = 3, m'_{F'} = -1\rangle$ and $|6^2P_{3/2} : F' = 3, m'_{F'} = 3\rangle$ [15]. Therefore the detection laser is about $\delta_1 = 2\pi \times 13.8MHz$ detuned from the transition $|1\rangle \rightarrow |6^2P_{3/2} : F' = 3, m'_{F'} = -1\rangle$, which yields a maximal ratio $(\Gamma_1/2\delta_1)^2 I(r)/I(0) \lesssim 9 \times 10^{-5}$ [15] between the photon scattering on non-target and target atoms. The impact on non-target atoms in the detection process may therefore be neglected.

Finally, we notice that the single qubit rotation may also be performed using a two-photon Raman transition [19] with the assistance of focused lasers. In this case, the beam waist widths of the Raman pulses needs to be relatively large such as $2\mu m$ so that small misalignment of the laser do not cause large changes of the laser intensity on the target atoms that may diminish the fidelity of the single qubit rotation. Because the two-photon Raman transitions only affect atoms inside the Rabi pulses, atoms separated by a long distance may be addressed simultaneously, which may reduce the total computation time.

In summary, we have analyzed a scheme for manipulating and measuring quantum states of single atoms in optical lattices with the assistance of focused lasers. With properly chosen experimental parameters, various manipulation errors are suppressed below 10^{-4} except the spontaneous emission probability of atoms in focused lasers. Our proposal includes a realistic and practical quantitative analysis suggesting plausible experimental implementation of single atom manipulation in optical lattice quantum computation architecture.

We thank V. Scarola for valuable discussion. This work is supported by ARDA, ARO, NSA-LPS.

- [1] M.A. Nielsen, and I.L. Chuang, *Quantum computation and quantum information*, (Cambridge University Press, Cambridge 2000).
- [2] P. Zoller, *et. al.*, arXiv: quant-ph/0405025.
- [3] D. Jaksch, *et. al.*, Phys. Rev. Lett. **82**, 1975 (1999).
- [4] O. Mandel, *et. al.*, Phys. Rev. Lett. **91**, 010407 (2000); Nature **425**, 937 (2003); O. Mandel, PhD dissertation.
- [5] L.-M. Duan, E. Demler, and M.D. Lukin, Phys. Rev. Lett. **91**, 090402 (2003).
- [6] A.M. Steane, Rep. Prog. Phys. **61**, 117 (1998).
- [7] P.W. Shor, Phys. Rev. A **52**, R2493 (1995).
- [8] H.J. Briegel, *et. al.*, J. Mod. Opt. **47**, 415 (2000).
- [9] R. Scheunemann, *et. al.*, Phys. Rev. A **62**, 051801(R) (2000).
- [10] A. Barenco, *et. al.*, Phys. Rev. A **52**, 3457 (1995).

- [11] R. Raussendorf and H.J. Briegel, Phys. Rev. Lett. **86**, 5188 (2001).
- [12] S.L. Rolston, in *Proceedings of the 1st International Conference on Experimental Implementation of Quantum Computation*, (Rinton Press, Princeton, 2001).
- [13] M. Greiner, *et. al.*, Nature **415**, 39 (2002).
- [14] D. Schrader, *et. al.*, Phys. Rev. Lett. **93**, 150501 (2004).
- [15] H.J. Metcalf, and P. van der Straten, *Laser cooling and trapping*, (Springer-Verlag, New York 1999).
- [16] P.S. Jessen and I.H. Deutsch, Adv. At. Mol. Opt. Phys. **37**, 95 (1996).
- [17] Only transitions to $6P$ states are considered because the detunings to other states are much larger.
- [18] H.K. Cummins, *et. al.*, Phys. Rev. A **67** 042308 (2003).
- [19] D.D. Yavuz, *et. al.*, Phys. Rev. Lett. **96**, 063001 (2006).